Bioceramics for Musculoskeletal Regenerative Medicine: Materials and Manufacturing Process Compatibility for Synthetic Bone Grafts and Medical Devices

Ciro A. Rodriguez, Hernan Lara-Padilla, and David Dean

Contents

C. A. Rodriguez
Escuela de Ingeniería y Ciencias, Tecnológico de Monterrey, Monterrey, Mexico
e-mail: ciro.rodriguez@itesm.mx

H. Lara-Padilla
Departamento de Ciencias de la Energía y Mecánica, Universidad de las Fuerzas Armadas ESPE, Sangolquí, Ecuador
e-mail: hvlara@espe.edu.ec

D. Dean (✉)
Department of Plastic Surgery, The Ohio State University, Columbus, OH, USA
e-mail: David.Dean@osumc.edu

A. Ovsianikov et al. (eds.), *3D Printing and Biofabrication*, Reference Series in Biomedical Engineering, https://doi.org/10.1007/978-3-319-45444-3_22

Abstract

This chapter is focused on bioceramics for musculoskeletal regenerative medicine, with emphasis on material and manufacturing compatibility in the development of synthetic bone grafts. Bioceramics are classified into families depending on their relative bioactivity: passive, bioactive, and bioresorbable. Passive bioceramics, such as alumina and zirconia, are mainly used for load-bearing implants. Bioactive ceramics, such as bioactive glass, are useful to generate a strong bond between metallic surfaces and bone. Bioresorbable ceramics are applied to bone void filling and scaffolds for synthetic grafts. A description of bioceramics and their use in manufacturing processes is given, with major emphasis on techniques that may be useful in the fabrication of regenerative devices such as synthetic bone grafts. The manufacturing processes of interest are classified into molding, additive manufacturing, and coating techniques. The use of bioceramic-based scaffolds in bone repair animal models and clinical studies is reviewed. Finally, this chapter provides an outlook of future research directions for improved bioceramic use in synthetic bone grafts or regenerative skeletal devices.

1 Introduction

Ceramics are nonmetallic and inorganic solids (Kingery et al. 1976). The majority of ceramics are compounds of metals, metalloids, or nonmetals. Most frequently they are oxides, nitrides, and/or carbides. However, diamond and graphite are also classified as ceramics. Glass, not a solid in strict terms, is therefore considered a special type of ceramic. Semiconductors are also ceramics, although sometimes they are considered a separate family of materials (Carter and Norton 2007).

An alternative definition for ceramics is given by McColm: "Any of a class of inorganic, nonmetallic products which are subjected to a temperature of 540 °C or above during manufacture or use, including metallic oxides, borides, carbides, or nitrides, and mixtures or compounds of such materials" (McColm 2013). Thus, the study of ceramics encompasses a wide range of materials.

When used in biomedical applications, especially when placed inside the human body, ceramics are referred to as bioceramics. The relative bioactivity of a given type of bioceramic allows its classification into one of the three following broad families: passive, bioactive, and bioresobable ceramics (see Fig. 1).

Passive or nearly inert bioceramics show minor interaction with human tissues. The most widely used passive ceramics are formulations of alumina and zirconia.

In contact with human tissue, bioactive materials generate a specific biological response at the interface, often resulting in the formation a bond between the tissue and the material. Bioactive ceramics may also be resorbable. If the resorption byproducts are safe, they are referred to as bioresorbable ceramics. Examples of bioactive ceramics include glasses such as Bioglass®, glass-ceramics such as apatite-wollastonite (A/W), dense synthetic hydroxyapatite (HAP), and a variety of bioceramic composites. When implanted bioactive ceramics form a layer of hydroxy-carbonate

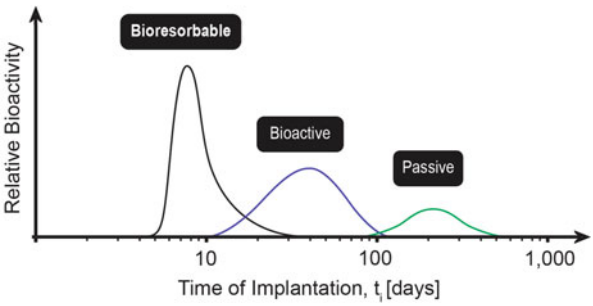

Fig. 1 Classification of bioceramics based on their relative bioactivity. Adapted from (Hench and Wilson 2013)

apatite (HCA), where collagen fibrils are incorporated, therefore binding the inorganic surface to the organic constituents of tissues (Hench and Wilson 2013). Bioresorbable ceramics include several calcium phosphates such as tricalcium phosphate (TCP) that degrades into calcium and phosphate salts (Hench and Wilson 2013).

1.1 Historic Perspective

In orthopedics, although the total hip replacement operation was first conducted in 1938, it was not until 1961 that much improved designs and materials made this procedure a clinical success (Learmonth et al. 2007). The use of alumina as a coating for the joint surface in hip implants was first attempted in the 1970s. Indeed, the current use of bioceramics as implant components is mostly limited to coatings, particularly for hip and knee implants. These coatings are an improvement over previous metal-on-metal joints and metal-bone interfaces (Semlitsch et al. 1977; Chevalier and Gremillard 2009). In the case of alumina coatings, it has been observed that they significantly reduce the generation of wear particles over previous metal-on-metal solutions (Hannouche et al. 2005). In order to improve the mechanical properties and reliability of hip implants, zirconia was also introduced as a candidate joint surface coating in the 1980s (Piconi and Maccauro 1999).

In its early use, approximately one of every six alumina- or zirconia-containing hip implants failed. With continuous improvement of alumina and zirconia, these materials today deliver much better ceramic coating-related failure rates in hip implant applications (i.e., less than 0.01%). The clinical success associated with the use of these advanced bioceramics has led to the implantation of millions of hip and knee total joint replacement devices worldwide (Chevalier and Gremillard 2009).

Feldspathic porcelain teeth and dentures were first introduced in the late 1700s in France. However, widespread use of porcelain in dentistry did not begin until the 1950s with new porcelain formulations that provided improved mechanical properties and affordable manufacturing procedures (Kelly et al. 1996). In addition to porcelain, alumina and zirconia are now widely used in dental applications.

In the 1960s, the development of bioactive ceramics began with the formulation of bioactive glass, commonly referred to as Bioglass® (Hench 2006). Systematic study of various bioresorbable synthetic calcium phosphates, such as hydroxyapatite

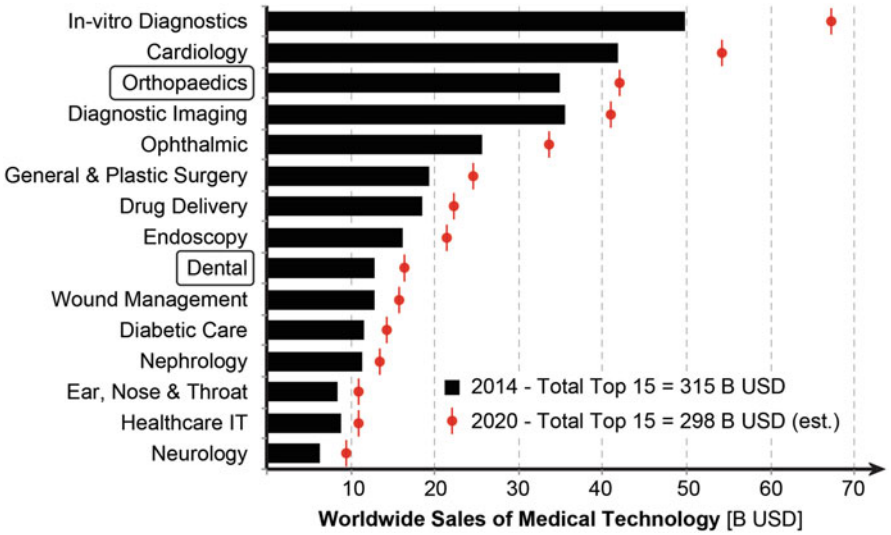

Fig. 2 Trends in worldwide sales of medical technology, considering the top 15 product categories (Evaluate 2015). The circled clinical fields indicate the best opportunities for bioceramics. Please note that many surgical fields other than orthopedics contribute to skeletal repair and regeneration. To that extent those therapies are equally good opportunities for bioceramic applications

and tricalcium phosphate, dates back to the 1980s (Best et al. 2008; Metsger et al. 1982). Today, industry provides a wide range of bone substitute products for use in non-weight-bearing defects. Most of these materials are composites that combine various calcium phosphates (Liu et al. 2013).

1.2 Markets

In regards to medical technology, bioceramics have a significant clinical and economic relevance (see Fig. 2). Orthopedics and dental applications are the mayor drivers in this field, with combined sales of $47.7 billion USD worldwide and significant projected growth in the next few years (Evaluate 2015).

2 Bioceramics and Manufacturing Process Compatibility

The complete scope of medical bioceramic uses includes a large number of material compositions and manufacturing processes. In order to provide a comprehensive map, Fig. 3 shows a general representation of material vs. manufacturing process compatibility.

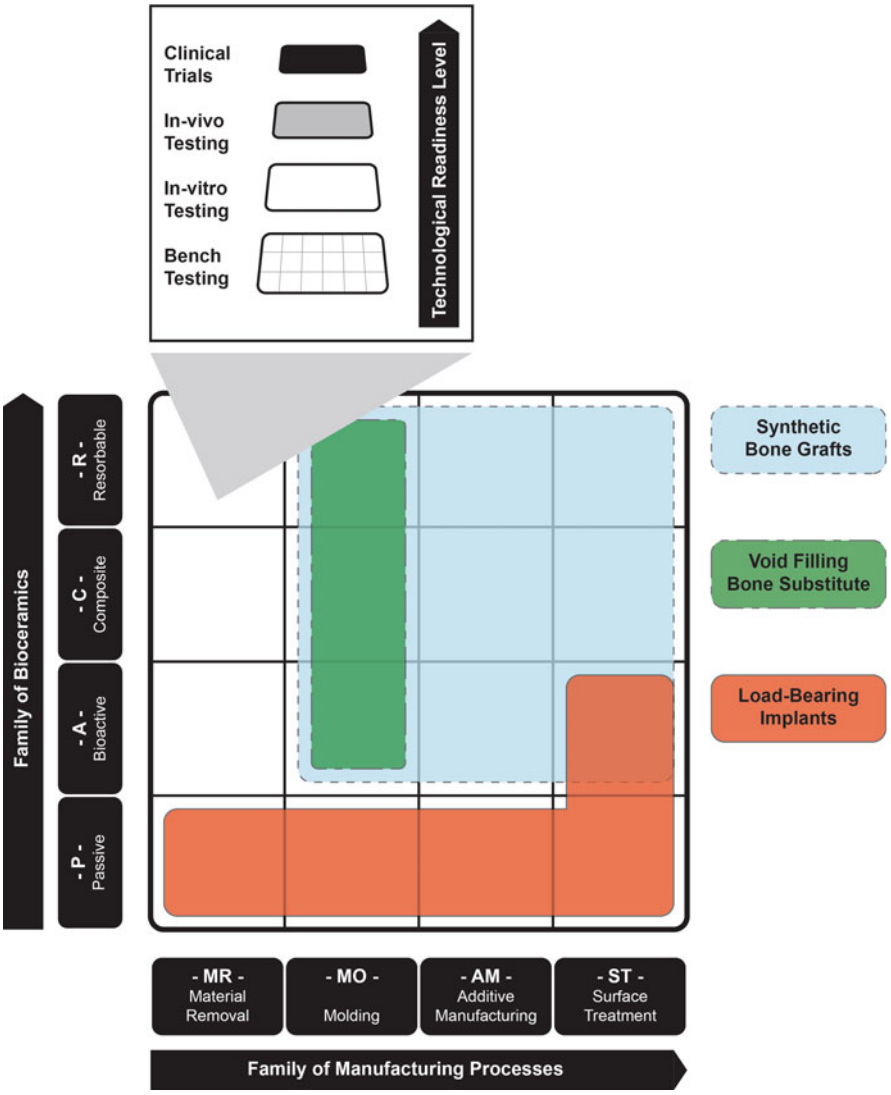

Fig. 3 Material vs. manufacturing process compatibility for bioceramics in musculoskeletal regenerative medicine

The forming of bioceramics involves manufacturing processes that utilize material removal (cutting and machining), molding, additive manufacturing, and surface treatments. In addition to the compatibility and process capability issues, there is also interest in mapping technology readiness levels of devices and current manufactur-

ing processes. This places each device in the continuum between proof-of-concept ideas and use in the clinic (i.e., bench to clinic progression) (Woodruff et al. 2012).

2.1 Load-Bearing Implants

Figure 4 shows the major application categories for bioceramics in musculoskeletal regenerative medicine. Load-bearing implants include components made mainly with passive bioceramics through material removal and molding processes. Bioactive ceramics are used as coatings or metallic components such as the stem or joint of

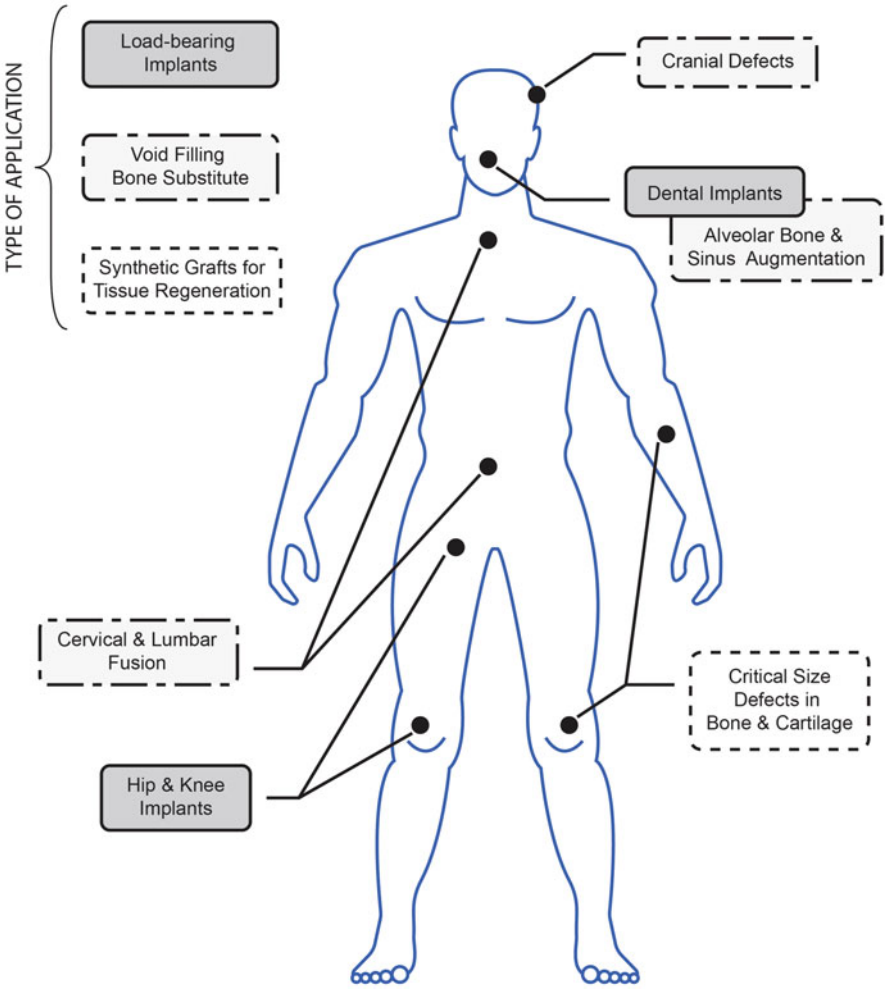

Fig. 4 Application of bioceramics in musculoskeletal regenerative medicine (Agarwal et al. 2009; Bartolo et al. 2012; Bonda et al. 2015; Obregon et al. 2015)

hip implants or the post, literally a bone screw, of a dental implant. Passive bioceramics can be processed via additive manufacturing processes but are more commonly used for product prototyping purposes than for the fabrication of clinical devices. Functional components require the close tolerance and surface finish capability of machining and grinding processes in order to minimize micro cracks and potential catastrophic failure.

2.2 Bone Substitutes for Void Filling

Bone substitutes for void filling may be manufactured with molding processes, using materials such as hydroxyapatite, tricalcium phosphate, or combinations of different bioceramics (see Fig. 3). These bone substitutes are available in the form of chips, granules, putties, or blocks that can be cut to fit a bone defect (Crowley et al. 2013). Some products are formulated with a matrix of collagen that contains a bioceramic phase (Pilipchuk et al. 2015).

When spinal fusion is indicated, the procedure involves: (a) removal of the disc, which in turn creates a void between adjacent vertebrae; (b) implantation of a spinal cage (a kind of spacer usually made from titanium alloy or high strength polymer such as PEEK); (c) stabilization with titanium screws and rods; and, finally, (d) filling the spinal cage with a bioceramic bone substitute. There are a number of products on the market, each with a specific formulation for spinal fusion and repair of fracture vertebrae (i.e., balloon kyphoplasty) procedures (Liu et al. 2013). Another major application of bone substitutes for void filling is related to dental extraction or periodontal diseases where teeth or jaw bone mass has been lost to the point that the deficient region cannot support dental implants. This bone supports the roots of the teeth and is therefore referred to as alveolar (i.e., tooth socket) bone. Repair and/or reconstruction of alveolar bone and or associated facial sinus augmentation procedures can involve the use of bioceramic bone fillers (Pilipchuk et al. 2015). Bone substitutes are also used to regenerate cavity defects left by tumors (Crowley et al. 2013) and repair small cranial defects (Bonda et al. 2015).

2.3 Synthetic Bone Grafts

Synthetic grafts are porous constructs, often shaped in the operating room, to a specific bone or cartilage defect. These synthetic grafts may include resorbable bioceramics that may act as a scaffold for cells and growth factors (Bonda et al. 2015). The synthetic bone graft category is a demanding application for bioceramics in musculoskeletal regenerative medicine. These materials have found limited clinical application in the repair of load-bearing defects.

The use of bioceramics in scaffolds as synthetic grafts can also be prepared as bioactive and bioresorbable ceramic composites. These composites can be fabricated with processes such as molding, additive manufacturing, or coating. The composite materials used for this type of scaffold may also be combined with polymers and

metals. Biphasic calcium phosphates are a widely studied composite that combine the properties of hydroxyapatite (HA; bioactive) and beta-tricalcium phosphate (β-TCP; bioresorbable) (Baradararan et al. 2012). The following sections will focus on synthetic bone graft materials and constructs, detailing the currently available bioceramics and manufacturing processes.

3 Synthetic Bone Grafts

Bone is a key component of the musculoskeletal system, providing structure for ambulatory and environmental manipulating functions, storing nutrients, protecting vital organs, and playing a key role in hematopoietic and immunological functions. Although bone possesses an extraordinary regenerative capacity, it can fail to heal under unstable and large deficit conditions. Defects in bone can be caused by trauma, cancer, congenital and developmental deformities, arthritis, aging, and infection (Larsen et al. 2015). In the trauma category alone, there is an estimate of 15 million fracture cases per year worldwide, with up to 10% of repairs subsequently having complications due to nonunion of large defects (Liu et al. 2013).

The standard of care treatment for nonreducible bone fractures (i.e., "reduction" of the gap caused by the break) and resections is an autologous bone graft, also referred to as autograft. Autografts are harvested from a donor site and implanted elsewhere in the same patient (Shrivats et al. 2014). Grafted bone has excellent osteogenic, osteoinductive, and osteoconductive properties. However, this approach also brings some important disadvantages: potential complications at the donor site (e.g., pain and morbidity), possibly a limited or insufficient blood supply, and often there is difficulty shaping the autograft to fit the bone defect (Crowley et al. 2013).

Another option is to seek bone via allogeneic graft (also referred to as allograft). Allografts are tissues harvested from human donors (i.e., people other than the patient), with subsequent graft processing for implantation in the patient. The main disadvantages of this approach are the risk of adverse immunological response (i.e., immunological rejection), potential disease transmission, and reduced osteogenic capacity due to devascularization, decellularization, demineralization, and/or sterilization processing. Xenografts are donor tissues derived from nonhuman species. Similar to allografts, these tissues are processed for sterility and biocompatibility. The risk of immunological response, disease transmission, and ethical issues associated with the use of animal tissues has limited the clinical use of xenografts (Shrivats et al. 2014).

The common clinical problem of bone defects and the limitations of current solutions (i.e., autografts, allografts, and xenografts) motivate an enthusiastic, worldwide search by the scientific community for alternatives to autologous or allogeneic bone grafts such as entirely synthetic bone graft strategies. Advances in bioceramics and manufacturing processes have opened a number of new paths for research and development into an artificial approach.

Early clinical applications of synthetic bone graft materials included scaffolds shaped from blocks of coral (primarily $CaCO_3$) (Pountos and Giannoudis 2016).

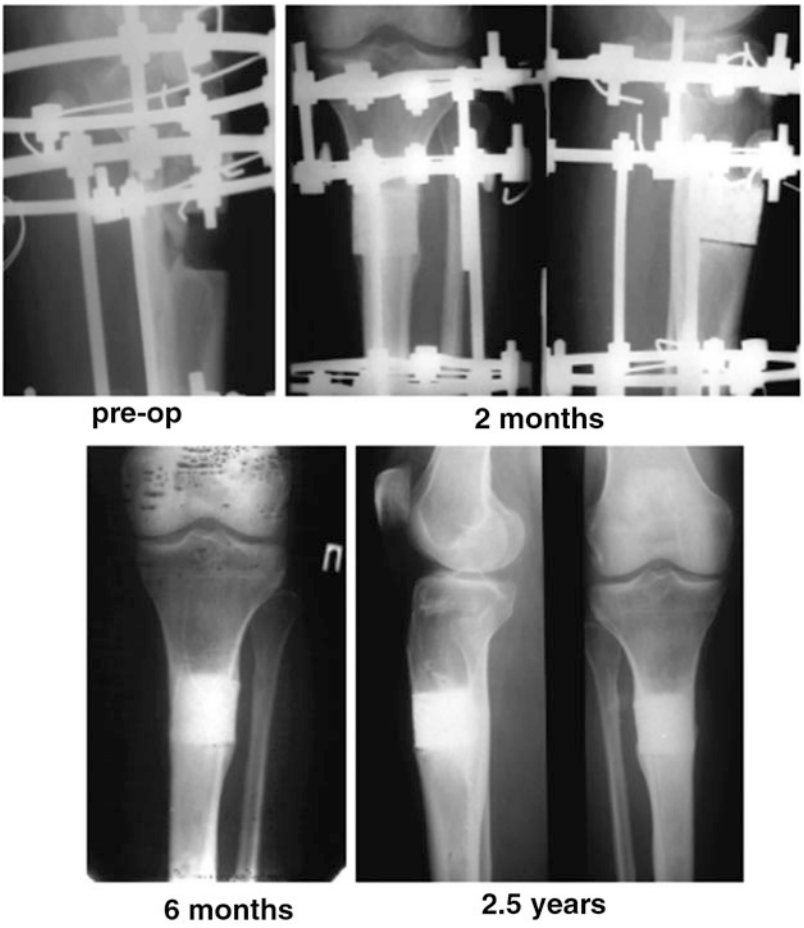

Fig. 5 Implantation of a porous bioceramic scaffold seeded with autologous BM-MSCs for clinical treatment of critical size segmental tibial defect (Marcacci et al. 2007)

Similarly, porous hydroxyapatite blocks with 60% interconnected porosity and an apparent density of 1.26 g/cm^3 have been studied. Autologous bone marrow-derived mesenchymal stem cells (BM-MSC) were expanded in vitro and seeded by capillarity into the scaffold. A pre-operative radiograph shows a 40 mm gap in the bone (see Fig. 5). After 2.5 years, much of the synthetic HAP was evident indicating an extremely slow resorption rate (Quarto et al. 2001; Marcacci et al. 2007).

The tissue engineering approach to bone repair studied by Marcacci et al. still has had limited clinical application due to a number of challenges (Cancedda et al. 2007). However, that clinical experience, together with numerous studies with animal models, can lead to a more systematic approach to the development of synthetic bone grafts (Crowley et al. 2013; Li et al. 2015).

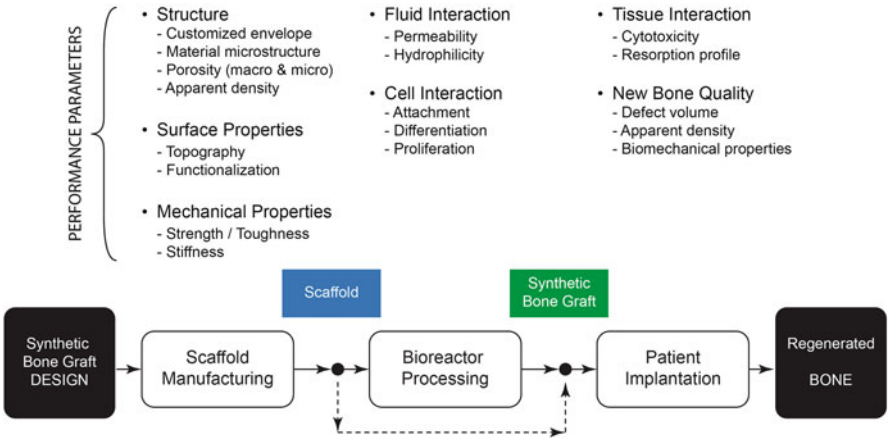

Fig. 6 Tissue engineering process for bone repair based on synthetic bone grafts

Another potentially promising process for the generation of a synthetic bone graft is outlined in Fig. 6. Studies have attempted to capture key performance parameters of the process at each stage. Based on the type of bone defect repaired, the starting point will be synthetic bone graft design. At the next stage, a scaffold is manufactured. The following stage involves combining cells with the scaffold to constitute a synthetic bone graft. Growth factors (bioactive molecules) may be added at this stage. For some cases, the scaffold alone (i.e., cell-free) is used as the graft. Finally, the synthetic bone graft is implanted into the bone defect to help regenerate new tissue.

Ultimately, we are interested in the quality of the newly regenerated bone. Neobone quality is measured in terms of the regenerated volume compared to the original bone defect size, the new bone's apparent density and its biomechanical properties. The final bone quality will depend on a complex interaction between the defect's wound healing and remodeling response and the synthetic bone graft material over time. Remodeling is necessary for the production/regeneration of strong bone. Nonresorbing material that does not degrade within 4–12 months may block this process.

It is clear that much research is still needed to understand and model the bone repair process (Larsen et al. 2015). However, a systematic approach to this challenge calls for defining and controlling key performance parameters at the different stages of graft fabrication and the healing response.

3.1 Morphology and Mechanical Properties of Scaffolds

In the context of synthetic bone grafts, the morphology and quality of scaffolds requires standard and comparable parameters. Figure 7 shows examples of this type of scaffold.

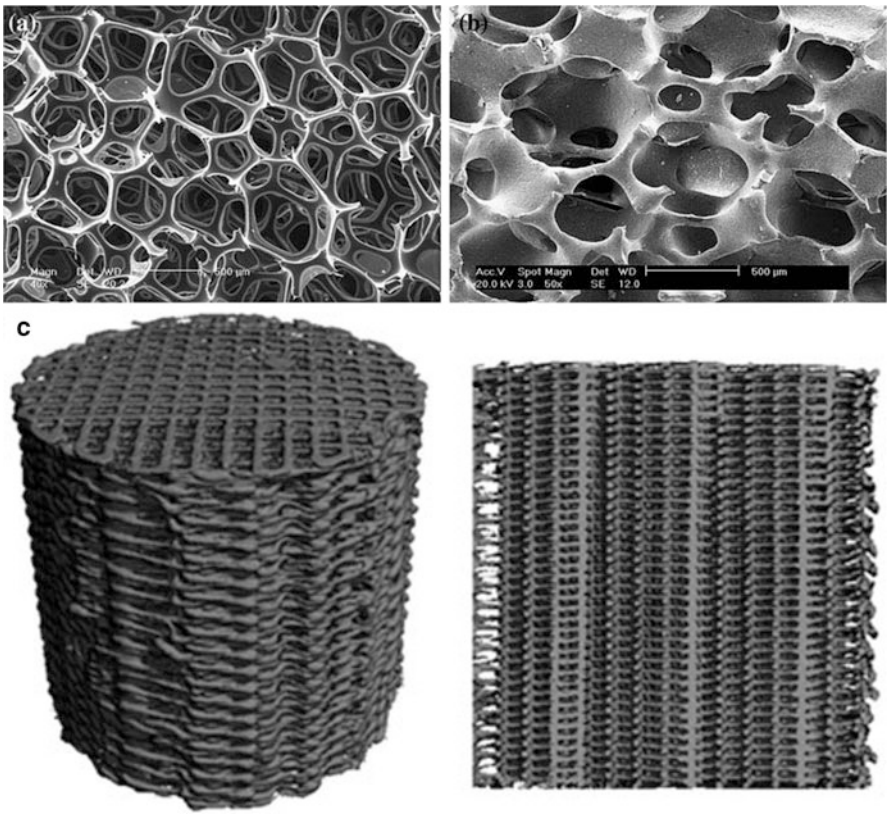

Fig. 7 Examples of scaffolds generated via molds and additive manufacturing (3D printing): (a) polyurethane foam (Cai et al. 2009), (b) scaffold from β-TCP/BG with 75% porosity (after sponge impregnation using the polyurethane foam as template and sintering), (c) micro tomography reconstruction of scaffold from composite of PCL and TCP, using fused deposition modeling (FDM) for processing (Reichert et al. 2011)

Total scaffold porosity (Π_{total}) is defined as a combination of the open or macroporosity (Π_{macro}) and the internal or microporosity (Π_{micro}) of the base material, as follows:

$$\Pi_{total} = \Pi_{macro} + \Pi_{micro} \quad (1)$$

When designing a scaffold, macroporosity (with dimensions over 100 microns) should be interconnected to allow flow (e.g., influx of nutrients and chemical signals and removal of waste products) during the osteogenic process. Porosity, tortuosity, hydrophilicity, and microporosity will all have an effect on scaffold permeability and its ability to guide new tissue formation. Some of the manufacturing processes for bioceramics produce an inherent microporosity (i.e., dimensions between

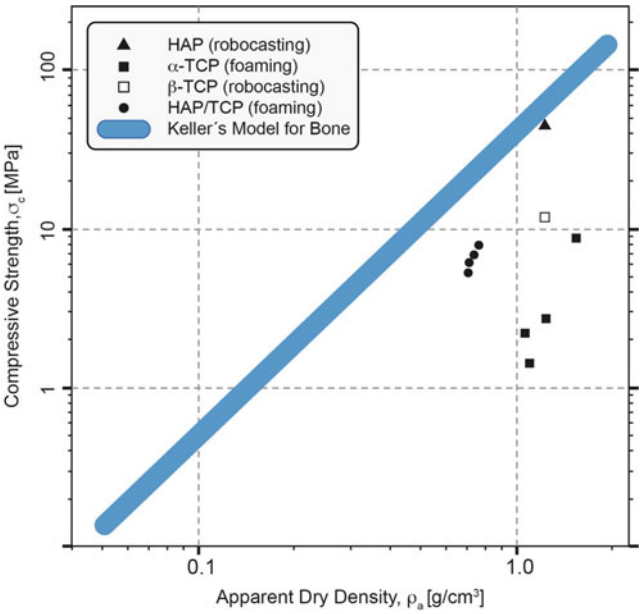

Fig. 8 Compressive strength vs. apparent dry density for bone and bioceramics-based scaffolds (Almirall et al. 2004; Baradararan et al. 2012; Keller 1994; Miranda et al. 2008)

100 nanometers and a few microns). Microporosity is not interconnected in these constructs. Some authors refer to the base material microporosity as "strut porosity" (Hing et al. 2005).

Total scaffold porosity (Π_{total}) is related to the apparent dry density (ρ_a) as follows:

$$\Pi_{total} = (1 - \rho_a/\rho_m) * 100\% \quad (2)$$

where the base material theoretical density is represented by ρ_m.

The apparent dry density of bone has been closely correlated to its mechanical properties, such as compressive strength and elastic modulus (see Fig. 8) (Keller 1994). Similarly, any comparison of bioceramic scaffolds and a manufacturing process should consider the mechanical properties as a function of apparent dry density.

A synthetic bone graft is intended to facilitate the regeneration and remodeling of bone. While performing this function, the graft should gradually resorb in response to bone formation. For many critical size defects, the adjacent bone segments would require stabilization with metallic plates or a rod during this process. Therefore, in this context, the ideal mechanical properties of the scaffold are not necessarily those of the healthy bone, but rather what is needed for bone regeneration. However, in terms of standardized parameters, it is useful to rate mechanical performance of scaffolds relative to each other and relative to Keller's Model for resilient bone (see Fig. 8).

3.2 Bioceramics and Manufacturing Process Compatibility

3.2.1 Bioceramic Devices Produced in Molds

Scaffolds for bone regeneration with interconnected porous structure can be produced in molds using a variety of methods, such as sponge impregnation, freeze drying, phase inversion, sol-gel foaming, particulate leaching, injection molding, and direct casting.

In the sponge impregnation method, a polyurethane foam template is impregnated with bioceramic slurry. The objective is to generate a thick coating of bioceramic slurry around the struts of the template. After drying the impregnated sponge, a sintering process is used to remove the polymer leaving behind the intended interconnected porous structure (Dai et al. 2015; Zreiqat et al. 2010).

Freeze drying, thermally induced phase inversion, and sol-gel foaming involve chemical reactions that produce a porous structure (Guo et al. 2012; Midha et al. 2013; Tamjid and Simchi 2015; Wang et al. 2007). Particulate leaching is based on a mixture of bioceramic material and a salt that is either compacted within a mold or poured into a mold. In a second step, the salt particulates are leached with water to form a porous structure (Zhang et al. 2016). The size, shape, concentration, and distribution of the particulate can be important. However, the resulting pore geometry cannot insure interconnectivity.

Injection molding requires a special mold with multiple cores and slides (i.e., moving components of the mold) that generate an interconnected geometry (Vivanco et al. 2012). In direct casting, a core (sometimes referred to as a "negative mold") is used to form the complete interconnected network of macropores. Then, a ceramic slurry is cast around the core (Li et al. 2013). Only injection molding and direct casting can use a mold to produce a designed structure that includes macroporosity. All other molding techniques tend to deliver a random distribution of interconnected macropore diameters, in a foam-like structure (see Fig. 7).

When the material for the scaffold is only bioceramic, a sintering process can be used to achieve a microstructure with good mechanical properties. The sintering step is itself a complex process that involves a number of parameters and requires optimization (Champion 2013). In general, an increased sintering temperature reduces microporosity and the resorption rate of the bioceramic scaffold (Yuan et al. 2010).

In terms of materials, some of the most promising advances involve processing composites that combine bioceramics and polymers through molding processes. In vivo testing with rats and rabbits were recently reported with this approach: freeze drying (Park et al. 2016; Chiba et al. 2016), compression molding, and particle leaching (Zhang et al. 2016), followed by phase inversion (Guo et al. 2012). More details about these studies can be found in the appendix.

The work reported by Chiba et al. uses octacalcium phosphate with gelatin. The scaffolds were tested on Japanese white rabbits with cavity tibial defect. Biomechanical testing of neobone was conducted with an indentation test, reaching near 100% of the compressive load compared to control cortical bone (Chiba et al. 2016).

The composite used by Zhang et al. combines HAP and PLLA/PLGA. They tested this material in a Sprague-Dawley rat calvarial defect (i.e., 6 mm round defect) model. After 12 weeks of implantation, an indentation test shows that new bone has obtained 85% of the hardness and 78% of the elastic modulus, compared to natural rat cranial bone. In this case, the scaffold had 80% macro porosity, with average pore size of 145 μm and compressive strength of 0.1 MPa.

Recently, the use of bioactive glass has been studied as a scaffold in in vivo studies utilizing rabbit, goat, dog, and sheep models (El-Rashidy et al. 2017). Selected animal studies with emphasis on biomechanical properties include rabbits (Tang et al. 2016) and goats (Ghosh et al. 2008). Tang et al. shows excellent biomechanical properties of new bone in rabbit radius segmental defect (16 mm), utilizing bioactive glass scaffolds manufactured by the sponge impregnation technique and BMP-2 (Bone Morphogenetic Protein).

A summary of selected in vivo studies using molding processes for scaffolds is shown in Table A.1. The studies are classified based on the bioceramic family and manufacturing process.

3.2.2 Additive Manufacturing Methods

Additive manufacturing (3D printing) technologies provide a wide range of possibilities for the fabrication of bioceramic scaffolds that may then be useful as synthetic bone graft scaffolds, particularly with bioceramics as a printable material or component of a printable material. Table 1 shows the most common suitable additive manufacturing methods for bioceramic materials. Other references provide extensive and detailed description of additive manufacturing (Larsen et al. 2015; Pati et al. 2015; Raman and Bashir 2015). Here, we provide only brief descriptions of these technologies.

In addition to those additive manufacturing processes used to produce bioceramic scaffolds, there are significant advances in recent years in developing powder bed additive manufacturing for load-bearing passive bioceramics. Partial melting (SLS) and full melting (SLM) approaches use bioceramics in the form of powder or slurry to produce parts in a single step or multiple steps (i.e., postprocessing after additive manufacturing). In this field, the main challenges are the bioceramic powder's flowability during the 3D printing process and the final material's microstructure (Deckers et al. 2014; Sing et al. 2017; Zocca et al. 2015).

The most advanced applications of bioceramic scaffolds produced via additive manufacturing are summarized here through in vivo animal model studies. Scaffolds based on inkjet printing of tricalcium phosphate scaffolds have been tested with rat, mouse, goat, and dog models. These studies have tested the viability of these bone regeneration strategies (Tarafder et al. 2013; Inzana et al. 2014; Habibovic et al. 2008; Igawa et al. 2006, respectively). Hi concentrations of ceramic have been suspended and 3D printed in polycaprolactone (PCL) or poly(lactic-co-glycolic-acid) (PLGA) for extrusion 3D printing as a flexible material referred to as "hyper-elastic bone". This material presented promising results in a rat spine model (Jakus et al. 2016, 2017). More details about these studies can be found in the appendix.

Table 1 Additive manufacturing processes suitable for bioceramics, as discussed in ISO/ASTM 52900 (2015). Please see glossary for process column acronyms

ASTM category		Process	Description
Material extrusion	Material melting	FDM: Fused deposition modeling	Extrusion of thermoplastic material through a heated nozzle. Variations of FDM are LDM (low-temperature deposition modeling) and PED (precision extruding deposition)
		MES: Melt electrospinning	In this process, the extruded FDM filament is further stretched by an electrical field
	Pressure dispensing	PAD: Pressure assisted dispensing	Dispensing of hydrogels with pressure assistance (sometimes used for cell bioprinting)
		DIW: Direct ink writing/ robocasting	Dispensing of ceramic paste with pressure assistance
		ELS: Electrospinning	Stretching of polymer fibers through electrical field, after a polymer/solvent solution is injected through a needle
Powder bed fusion		SLS: Selective laser sintering	Sintering or partial melting of powder via laser without controlled atmosphere (i.e., variable humidity)
		SLM: Selective laser melting	Full melting of powder e-beam or via laser with controlled atmosphere
Binder jetting		3DP: Inkjet printing	Consolidation of powder material through binder jet
Vat photopolymerization		SLA: Stereolithography	Curing of photopolymer through UV laser
		DMD: Direct micromirror device	Curing of photopolymer through UV lamp and DLP mask

Recently, bioactive glass (processed by SLS) was used as a BMP-2 carrier and tested in rats with a femur segmental defect (5 mm) and stabilization with an internal rod (Liu et al. 2014). Biomechanical performance of the resulting neobone was assessed via a three point bending test.

Ceramic/metal composites have also shown promise as viable scaffold biomaterials for bone regeneration. Sun et al. report the use of direct ink writing of a paste made of Wollastonite (CSi) and magnesium for the fabrication of bone scaffolds. Rabbits with round calvarial defects (8 mm) were used in an in vivo model to test the viability of these scaffolds. The regenerated bone showed compressive strengths up to 45 MPa (Sun et al. 2016).

The use of larger animal models with critical size cranial, radial, femoral, or tibial segmental defects is common (e.g., rabbits, dogs, sheep, goats, pig, or horse models) once small mammal work, often with a mouse, guinea pig, or rat model, has shown biocompatibility and other aspects of safety and effectiveness. These larger mammal models are a more challenging test due to slower metabolism and wound healing as well as load-bearing, all of which are more like what is seen in a human patient. Recent studies with a sheep tibial segmental defect show some

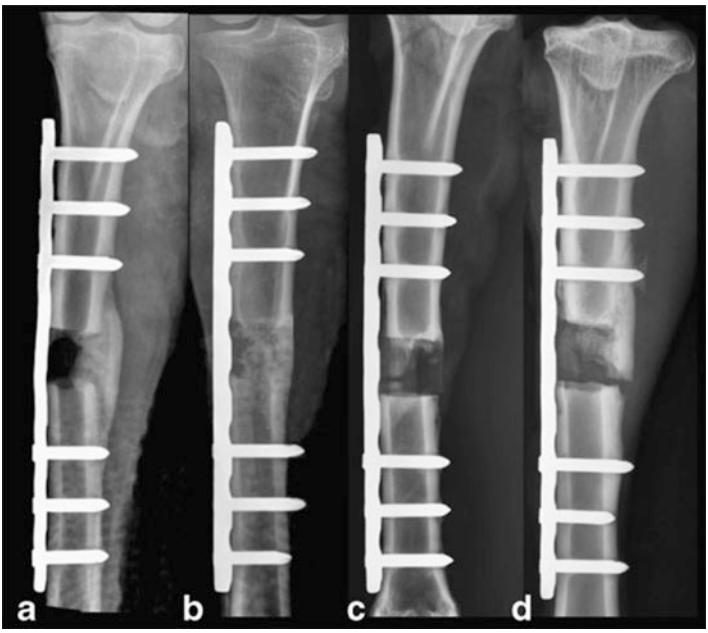

Fig. 9 Tibial segmental defect (20 mm) in sheep: (a) untreated defect, (b) autologous bone graft, (c) synthetic bone graft with mPCL-TCP scaffold, (d) synthetic bone graft with PDLLA-TCP-PCL scaffold (Reichert et al. 2011)

preliminary results with bioceramic bone scaffolds (Lohfeld et al. 2012; Reichert et al. 2011). Lohfeld et al. tested a composite scaffold composed of β-TCP + PCL (polycaptrolactone) powder (fabricated via SLS). Reichert et al. tested FDM 3D printed scaffolds composed of a composite of TCP and a resorbable polymer. By comparison with the mechanical properties of a (control) healthy tibia, the combination of medical grade PCL with TCP achieved 15% of the torsional moment, while the autologous bone graft showed 19% (sacrifice at 12 weeks post-implantation) (see Fig. 9). Abbah et al. tested an FDM-based scaffold for intervertebral fusion in a pig model with scaffolds combining β-TCP and PCL. They observed that the biomechanical properties of the fused vertebrae with a scaffold were similar to those of the autograft treatment (Abbah et al. 2009).

Other promising fabrication processes include electrospinning, which can be used to generate fine fibers with diameters in the micron and submicron range (Bartolo et al. 2012). Jaiswal et al. showed the viability of this process in bone regeneration by combining PLLA fibers and a coating of HAP and testing these composite scaffolds in vivo (Jaiswal et al. 2013). It is also possible to use electrospun fibers for drug delivery (Ji et al. 2011).

Eletrospun fibers can also be woven into defined or undefined meshes. The orientation of electrospun fibers is determined by the orientation of the fiber source and the cylindrical mandrel onto which those fibers are spun. Melt electrospinning

has been used to deposit polymer fibers with a diameter of about 30 μm, with embedded bioceramics, in a controlled manner. Therefore, a scaffold with controlled macroporosity, ceramic constituents, and/or a roughened texture can be fabricated with this process (Ren et al. 2014).

A summary of selected in vivo studies using additive manufacturing for scaffolds is shown in Table A.2. The studies are classified based on the bioceramic family and manufacturing process.

3.2.3 Surface Treatment Methods

The bioceramic-based surface treatment methods discussed here are limited to bioceramic coatings for scaffolds. In this case, a scaffold or another type of medical device is first generated through molding, CNC, or an additive manufacturing processe. Then, a coating is applied to improve functional properties of the device.

Recently, Li et al. report a baghdadite ($Ca_3ZrSi_2O_9$) scaffold (initially processed by sponge impregnation) with a coating of nano bioactive glass/PCL (coating processing by immersion). This scaffold was tested in a sheep tibial segmental defect (30 mm) model. A plate and a cast provided stabilization for the first 3 weeks of healing. After 3 weeks, only the cast is removed. Baghdadite scaffolds with and without the coating were tested. Normalized torsional test of the tibial diaphysis was conducted after 26 weeks of implantation, resulting in 5–10% torsional strength and 10–25% torsional stiffness compared with reference healthy tissue (Li et al. 2016).

In a different study, a PPF scaffold (3D printed by SLA [stereolithography, i.e., polymer photocrosslinking]) was coated with biphasic calcium phosphate (BCP), HAP only, or β-TCP only (by immersion). Different BMP-2 doses were used with each type of scaffold in a round rabbit calvarial defect (15 mm) model. After a 6-week implantation period, push-out testing was conducted (i.e., with a flat round indenter). There was no significant difference in volume of new bone among the different coatings (Dadsetan et al. 2015).

Nie et al. showed compressive strength of bioceramic scaffolds (sponge impregnation of BCP, with 94–97% macroporosity) coated with a composite of nanoHAP/PLLA cited as reaching the range of spongy bone in a rabbit femoral head defect (5 × 15 mm) (Nie et al. 2015). Qui et al. report on the use of a coated bioceramic scaffold for drug delivery in a rat calvarial defect model (6 mm) (Qiu et al. 2016).

Recently a different approach to delivering bioactive molecules involving ceramic coatings has been tried. Instead of infusing whole bioactive cytokines such as BMP-2 into the microporous spaces of a ceramic coating, a bioactive peptide, often the active site, or ligand, of a naturally occurring cytokine, is attached to a ceramic coating. The Becker laboratory has shown methods utilizing a catechol strategy for polymer (Policastro et al. 2015) and metal (Tang et al. 2014; Xu et al. 2017) substrates. More details about these studies can be found in the appendix.

A summary of selected in vivo studies using coating processes for medical device, is shown in Table A.3. These studies are classified based on the bioceramic material and manufacturing process.

4 Conclusions

The development of bioceramics has shown promise for contributing to musculoskeletal regenerative medicine. Bioceramic solutions have been found to reduce friction at joint surfaces in hip and knee joint replacement devices, which are recognized as standard-of-care practice. The use of bone substitutes for non-load-bearing skeletal void filling has spurred much research, but, to date, few clinical applications reliably use regenerative bioceramic materials for use in load-bearing skeletal segments with or without the assistance of metallic hardware (Kurien et al. 2013).

Thus, when it comes to taking advantage of the inherent properties of bioceramics for the construction of synthetic bone grafts to regenerate cortical bone, clinical translation has been more limited. The tissue engineering approach that combines scaffolds, cells, and signals (mainly in the form of growth factors) involves complex sets of interactions between synthetic materials and bone-wound healing and bone biology. Therefore, it is not surprising that the development of load-bearing synthetic bone graft strategies remains a technology gap area.

Next, we summarize some of the trends observed in our review of the study and use of bioceramic synthetic bone grafts materials.

4.1 High Resolution Manufacturing Processes and Composites

While bioceramic coatings have become very sophisticated, there remain tremendous challenges in improving bioceramic materials for use in traditional (e.g., grinding and molding) and advanced (e.g., electrospinning, additive manufacturing) fabrication processes. Early scaffold tested in animal models had relatively simple sources for porous spaces (i.e., uncontrolled, naturally formed, with imprecise porosity and permeability) macroporosity (Habibovic et al. 2008). As new additive manufacturing technologies were developed for ceramic powders, higher resolution and therefore more design flexibility can be achieved with processes like SLA (Elomaa et al. 2013; Zanchetta et al. 2016) and DMD (Digital Micromirror Device which houses a Digital Light Processing [DLP] chip; Felzmann et al. 2012; Tesavibul et al. 2012) photocrosslinking of polymer/ceramic resins. For example, the use of nano size particles and doping of ceramic material formulations with 3D printable polymer resins or metallic powders is being explored (Bose et al. 2013; Shao et al. 2016) for use in regenerative medical devices.

4.2 Graded Materials

Of the research and clinical cases reviewed here, all utilize uniform levels of macroporosity and microporosity throughout (Paderni et al. 2009; Li et al. 2016). Moreover, the relationship of geometry, material properties, and functions such as walking, manipulating the environment, or chewing are rarely considered in the

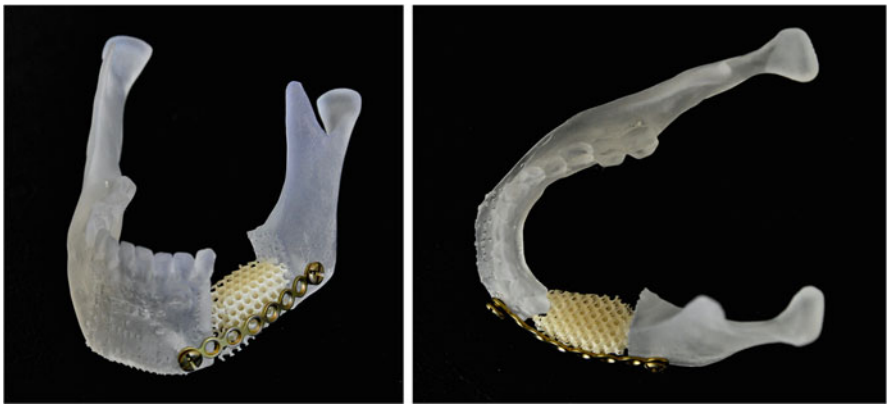

Fig. 10 Model simulating the regeneration of mandibular segmental with a synthetic bone graft and a stabilization plate that will be needed during the bone regeneration process

design of regenerative medical devices (an exception: Moghaddam et al. 2016a). The graded nature of natural bone structure suggests that graded material properties may better mimic the original structure and/or promote regeneration (Jahadakbar et al. 2016; Muller et al. 2015; Zhou et al. 2014). It may be useful to place more effort on the study of simultaneous restoration of shape and function as part of healthy tissue capable of maintaining both (see Fig. 10) (Moghaddam et al. 2016b).

4.3 Standardized In Vivo Testing

Currently, the research literature shows a wide range of animal models and testing methods. There is little discussion about the relationship of the model used to the intended therapy. It is likely that a generalized, load-bearing, bone substitute will have success in both small rodents and large mammal models. However, a large animal model will likely be more comparable to humans as critical size, cortical bone defects, of the size seen in humans are only available in mammals the size of rabbits and larger (Schmitz and Hollinger 1986). Rabbits are easy to handle but do not present any bone that is directly comparable to one that will be treated in human patients. Dogs are considered an appropriate model for some bones. Sheep, goats, horses, and pigs also provide some bones that are similar to the structures found in the human skeleton (Zoetis et al. 2003; Pearce et al. 2007). While nothing will replace the need for human clinical trials to accurately assess safety and efficacy, it is essential that these studies demonstrate the regeneration of biomechanically competent, critical size, fractures or segmental bone defects relevant to the intended human therapy.

Acknowledgments The authors acknowledge partial support from the Army, Navy, NIH, Air Force, VA, and Health Affairs to support the AFIRM II effort under award No. W81XWH-14-2-

0004. The US Army Medical Research Acquisition Activity is the awarding and administering acquisition office for award No. W81XWH-14-2-0004. Partial support was also provided by a Third Frontier (State of Ohio) Technology Validation and Startup Fund (TVSF) grant #15-791 grant, CONACyT grant #DCI from the Government of Mexico to Hernan Lara Padilla, and CONACyT #grant #274867 from the Mexican Government to Ciro A. Rodriguez.

Glossary

3DP Inkjet printing (type of additive manufacturing process)
BCP Biphasic calcium phosphate
BG Bioactive glass
CaP Calcium phosphate
CSF Calcium sulfate ($CaSO_4$)
DCS Dicalcium silicate (Ca_2SiO_4)
DIW Direct ink writing/robocasting (type of additive manufacturing process)
DLP Digital light processing (type of additive manufacturing process)
DMD Direct micromirror device (type of additive manufacturing process)
ELS Electrospinning (type of additive manufacturing process)
FDM Fused deposition modeling (type of additive manufacturing process)
HAP Hydroxyapatite
LDM Low-temperature deposition modeling (type of additive manufacturing process)
MES Melt electrospinning (type of additive manufacturing process)
nHA Nano-hydroxyapatite
OCP Octacalcium phosphate ($Ca_8H_2(PO_4)_6{\cdot}5H_2O$)
PA Polyamide
PAD Pressure assisted dispensing (type of additive manufacturing process)
PCL Polycaprolactone
PED Precision extruding deposition (type of additive manufacturing process)
PLA Polylactide acid
PLDLLA Poly(L-lactide-co-D,L-lactide)
PPF Poly(propylene fumarate)
SLA Stereolithography (type of additive manufacturing process)
SLM Selective laser melting (type of additive manufacturing process)
SLS Selective laser sintering (type of additive manufacturing process)
Slide In the design of injection molds, slides are moving components
Sr-HT Sr-hardystonite (Sr-$Ca_2ZnSi_2O_7$)
TCP Tricalcium phosphate
TTCP Tetracalcium phosphate ($Ca_4(PO_4)_2O$)

Appendix

See Tables A.1 to A.3.

Table A.1 Molding processes for bioceramic-based scaffolds (selected studies with in vivo testing)

		Scaffold					In vivo testing		
		Mfg. process	Type of bioactive bioceramic	Macro porosity, Π_{macro} [%]	Pore diameter, D_p [μm]	Compressive strength, σ_c [MPa]	Type of animal model	New bone evaluation	Reference
Bioceramic family	Bioresorbable	Phase inversion (solver: polyvinyl alcohol)	β-TCP	37.0	8–150	24.5* *Flexural strength	Bengal goat with cavity radius defect (10×5 mm^2)	Histology Biomechanical testing: push out (no natural tissue control)	Ghosh et al. 2008
	Composite	Freeze drying	Silk fibroin + β-TCP	–	50	0.7	Sprague-Dawley rats with round calvarial defect (4 mm) Implantation period: 8 weeks	Histology Qualitative microCT	Park et al. 2016
			Gelatin + OCP	–	10–500	–	Japanese white rabbits with cavity tibial defect (6 mm in diameter) Implantation period: 8 weeks	Histology Biomechanical testing: push-out test (control with normal tissue)	Chiba et al. 2016
		Compression molding (NaCl particles 100–200 μm in diameter and distilled water leaching)	PLLA/ PLGA + hap	80	145	0.9	Sprague-Dawley rats with round calvarial defect (6 mm) Implantation period: 6 & 12 weeks	Bone density Biomechanical testing: indentation hardness (control with normal tissue)	Zhang et al. 2016

(*continued*)

Table A.1 (continued)

		Scaffold					In vivo testing		
		Mfg. process	Type of bioactive bioceramic	Macro porosity, Π_{macro} [%]	Pore diameter, D_p [μm]	Compressive strength, σ_c [MPa]	Type of animal model	New bone evaluation	Reference
		Phase inversion (solvent: ethanol)	PA + HAP	81	100–500	4.4	New Zealand white rabbits with rectangular mandibular angle and body defect (15 × 8 mm). 2, 4, & 12 weeks	Histology MicroCT for new bone volume	Guo et al. 2012
			PA + nHA	52–70	50–500	13.2–33.9	New Zealand white rabbits with rectangular mandibular defect (8 × 12 mm) Implantation period: 2, 4, 8 & 12 weeks	Histology (new bone volume estimation)	Wang et al. 2007
	Bioactive	Sol-gel foaming	BG	93	100–500	–	Wistar male rats with cavity tibial defect (3 mm) Implantation period: 11 weeks	MicroCT for new bone volume	Midha et al. 2013
		Phase inversion (solver: polyvinyl alcohol)	HAP BG	35.2 38.6	6–164 14–160	42.20* 6.70* *Flexural strength	Bengal goat with cavity radius defect (10 × 5 mm^2)	Histology Biomechanical testing: push out (no natural tissue control)	Ghosh et al. 2008

			BG	38.6	14–160	–	Bengal goat with cavity radius defect ($12 \times 5 \times 3$ mm^3)	Histology Radiological examination	Nandi et al. 2009
		Sponge impregnation (template: Polyurethane foam)	β-DCS	53–71	300	10.4–28.1	Mice as incubators in subcutaneous scaffold implantation Implantation period: 9 weeks	Histology	Dai et al. 2015
			Sr-HT	78	–	2.2	Wistar female rats with cavity tibial defect (3×3 mm) Implantation period: 3 & 6 weeks	Histology Histomorphometry	Zreiqat et al. 2010
			BG	60–90	–	0.64–4.28 MPa	New Zealand rabbit with radius segmental defect (16 mm) Implantation period: 2 & 4 weeks	MicroCT: new bone volume Biomechanical testing: three point bending (normal tissue as control).	Tang et al. 2016

BG bioactive glass, *DCS* dicalcium silicate (Ca_2SiO_4), *HAP* hydroxyapatite, *nHA* nano-hydroxyapatite, *OCP* octacalcium phosphate ($Ca_8H_2(PO_4)_6{\cdot}5H_2O$), *PA* polyamide, *PCL* polycaprolactone, *Sr-HT* Sr-Hardystonite (Sr-$Ca_2ZnSi_2O_7$), *TCP* tricalcium phosphate

Table A.2 Additive manufacturing processes for bioceramic-based scaffolds (selected studies with in vivo testing)

		Scaffold					In vivo testing		
		Mfg. process	Bioceramic	Macro porosity, Π_{macro} [%]	Pore diameter, D_p [μm]	Compressive strength, σ_c [MPa]	Type of animal model	New bone evaluation	Reference
Bioceramic family	Bioresorbable	3DP	β-TCP	32–43/ 28–40/ 24–35	500/750/ 1000	5–11/5–6/ 4–5	Sprague–Dawley rats with femur cavity defect (3 mm) Implantation period: 2 weeks	Histology	Tarafder et al. 2013
		3DP	TCP	–	1300	8.3–21.7	Dutch milk goats with decorticated transverse processes of the vertebrae Implantation period: 12 weeks	Histology	Habibovic et al. 2008
		3DP	α-TCP	61	2000	18.6	Beagle dogs with square calvarial defect Implantation period: 24 weeks	Histology	Igawa et al. 2006
	Composite	3DP	HAP + α-TCP	22–45	30–150	–	Female BALB/cJ mice with femoral segmental defect (2 mm). Stabilization: PEEK plate Implantation period: 9 weeks	MicroCT Biomechanical testing: torsional strength (treatment with allograft as control)	Inzana et al. 2014

		DIW	CSi + Mg	60–63	–	40.0–65.0	Rabbit with round calvarial defect (8 mm) Implantation period: 12 weeks	Histology (new bone area estimation) Biomechanical testing: compressive strength (no natural tissue as control)	Sun et al. 2016
		SLS	β-TCP + PCL	68	–	–	Female mountain sheep with segmental tibial defect (20 mm). Stabilization: plate and cast for implantation duration. Implantation period: 14 weeks	Histology Peripheral quantitative computed tomography scanner for bone density Biomechanical testing: three-point bending stiffness (natural tissue as control)	Lohfeld et al. 2012
		FDM	a: mPCL + TCP b: PLDLLA + TCP + PCL	71 (a) 44 (b)	350–500	–	Merino sheep with segmental tibial defect (20 mm). Stabilization: titanium plate Implantation period: 12 weeks	MicroCT for new bone volume Biomechanical testing: torsional strength and stiffness (natural tissue as control)	Reichert et al. 2011

(*continued*)

Table A.2 (continued)

		Scaffold					In vivo testing		
		Mfg. process	Bioceramic	Macro porosity, Π_{macro} [%]	Pore diameter, D_p [μm]	Compressive strength, σ_c [MPa]	Type of animal model	New bone evaluation	Reference
		FDM	β-TCP + PCL	70	350–500	–	SPF Yorkshire pig with removal of intervertebral disk Implantation period: 6 months	Histology hismorphometry. MicoCT: new bone volume Biomechanical testing: lateral bending and axial rotation (intact disk as control)	Abbah et al. 2009
	Bioactive	SLS	BG	Cylinder with four side though holes		40	Long-Evans male rats with femur segmental defect (5 mm) Stabilization: Internal rod (1.6 mm diameter) Implantation period: 15 weeks	Radiology scoring Biomechanical testing: three-point bending (no natural tissue as control)	Liu et al. 2014

BG bioactive glass, *CaP* calcium phosphate, *CSF* calcium sulfate ($CaSO_4$), *HAP* hydroxyapatite, *PCL* polycaprolactone, *PLA* polylactide acid, *PLDLLA* poly (L-lactide-co-D,L-lactide), *TCP* tricalcium phosphate, *TTCP* tetracalcium phosphate ($Ca_4(PO_4)_2O$)

Table A.3 Coatings for bioceramic-based for scaffolds (selected studies with in vivo testing)

		Scaffold					In vivo testing		
		Mfg. process	Coating bioceramic	Substrate	Macro porosity, Π_{macro} [%]	Pore diameter, D_p [μm]	Type of animal model	Performance	Reference
Bioceramic family	Bioresorbable	Immersion	BCP	PPF (SLA)	39	429	New Zealand white rabbits with round calvarial defect (15 mm) Implantation period: 6 weeks	MicroCT for new bone volume Biomechanical testing: push-out test (no control with natural tissue)	Dadsetan et al. 2015
	Composite	Immersion	PCL + nBG	Baghdadite (sponge impregnation + sintering)	75–77	–	Merino wethers with segmental tibia defect (30 mm) Stabilization: plate and cast for 3 weeks Implantation period: 6 weeks	MicroCT for new bone volume Biomechanical testing normalized torsional testing (natural tissue as control)	Li et al. 2016
		Immersion	Mg-substituted β-TCP	PPF (SLA)	40	354	New Zealand white rabbits with round calvarial defect (15 mm) Implantation period: 6 weeks	MicroCT for new bone volume Biomechanical testing: push-out test (no control with natural tissue)	Dadsetan et al. 2015

(*continued*)

Table A.3 (continued)

		Scaffold					In vivo testing		
		Mfg. process	Coating bioceramic	Substrate	Macro porosity, Π_{macro} [%]	Pore diameter, D_p [μm]	Type of animal model	Performance	Reference
		Immersion	PLLA/nHA	BCP (sponge impregnation + sintering)	94–97	300–600	Japanese rabbits with cavity femur head defect (5 × 15 mm)	Histology	Nie et al. 2015
	Bioactive	Eletrophoretic deposition	Mesoporous silica nanoparticles	PLLA/PCL (thermally induced phase separation)	–	–	Sprague-Dawley male rats with round calvarial defect (6 mm)	Qualitative analysis with microCT	Qiu et al. 2016
		Immersion	Carbonated HAP	PPF (SLA)	39	403	New Zealand white rabbits with round calvarial defect (15 mm) Implantation period: 6 weeks	MicroCT for new bone volume Biomechanical testing: Push-out test (no control with natural tissue)	Dadsetan et al. 2015

BCP biphasic calcium phosphate, *HAP* hydroxyapatite, *nHA* nano-hydroxyapatite, *PCL* polycaprolactone, *PPF* poly(propylene fumarate), *PLA* polylactide acid

References

Abbah SA, Lam CXL, Hutmacher DW, Goh JCH, Wong H-K (2009) Biological performance of a polycaprolactone-based scaffold used as fusion cage device in a large animal model of spinal reconstructive surgery. Biomaterials 30:5086–5093

Agarwal R, Williams K, Umscheid CA, Welch WC (2009) Osteoinductive bone graft substitutes for lumbar fusion: a systematic review. J Neurosurg Spine 11:729–740

Almirall A, Larrecq G, Delgado J, Martínez S, Planell J, Ginebra M (2004) Fabrication of low temperature macroporous hydroxyapatite scaffolds by foaming and hydrolysis of an α-TCP paste. Biomaterials 25:3671–3680

Baradararan S, Hamdi M, Metselaar IH (2012) Biphasic calcium phosphate (BCP) macroporous scaffold with different ratios of HA/β-TCP by combination of gel casting and polymer sponge methods. Adv Appl Ceram 111:367–373

Bartolo P, Kruth J-P, Silva J, Levy G, Malshe A, Rajurkar K, Mitsuishi M, Ciurana J, Leu M (2012) Biomedical production of implants by additive electro-chemical and physical processes. CIRP Ann Manuf Technol 61:635–655

Best SM, Porter AE, Thian ES, Huang J (2008) Bioceramics: past, present and for the future. J Eur Ceram Soc 28:1319–1327

Bonda DJ, Manjila S, Selman WR, Dean D (2015) The recent revolution in the design and manufacture of cranial implants. Neurosurgery 77:814–824

Bose S, Fielding G, Tarafder S, Bandyopadhyay A (2013) Understanding of dopant-induced osteogenesis and angiogenesis in calcium phosphate ceramics. Trends Biotechnol 31:594–605

Cai S, Xu GH, Yu XZ, Zhang WJ, Xiao ZY, Yao KD (2009) Fabrication and biological characteristics of β-tricalcium phosphate porous ceramic scaffolds reinforced with calcium phosphate glass. J Mater Sci Mater Med 20:351–358

Cancedda R, Giannoni P, Mastrogiacomo M (2007) A tissue engineering approach to bone repair in large animal models and in clinical practice. Biomaterials 28:4240–4250

Carter B, Norton G (2007) Ceramic Materials. Springer, New York, pp 3–6

Champion E (2013) Sintering of calcium phosphate bioceramics. Acta Biomater 9:5855–5875

Chevalier J, Gremillard L (2009) Ceramics for medical applications: a picture for the next 20 years. J Eur Ceram Soc 29(7):1245–1255

Chiba S, Anada T, Suzuki K, Saito K, Shiwaku Y, Miyatake N, Baba K, Imaizumi H, Hosaka M, Itoi E, Suzuki O (2016) Effect of resorption rate and osteoconductivity of biodegradable calcium phosphate materials on the acquisition of natural bone strength in the repaired bone. J Biomed Mater Res A 104:2833–2842

Crowley C, Wong JM-L, Fisher DM, Khan WS (2013) A systematic review on preclinical and clinical studies on the use of scaffolds for bone repair in skeletal defects. Curr Stem Cell Res Ther 8:243–252

Dadsetan M, Guda T, Runge MB, Mijares D, Legeros RZ, Legeros JP, Silliman DT, Lu L, Wenke JC, Brown Baer PR, Yaszemski MJ (2015) Effect of calcium phosphate coating and rhBMP-2 on bone regeneration in rabbit calvaria using poly(propylene fumarate) scaffolds. Acta Biomater 18:9–20

Dai Y, Liu H, Liu B, Wang Z, Li Y, Zhou G (2015) Porous β-Ca2SiO4 ceramic scaffolds for bone tissue engineering: in vitro and in vivo characterization. Ceram Int 41:5894–5902

Deckers J, Vleugels J, Kruth JP (2014) Additive manufacturing of ceramics: a review. J Ceram Sci Technol 5:245–260

Elomaa L, Kokkari A, Närhi T, Seppälä JV (2013) Porous 3D modeled scaffolds of bioactive glass and photocrosslinkable poly(ε-caprolactone) by stereolithography. Compos Sci Technol 74:99–106

El-Rashidy AA, Roether JA, Harhaus L, Kneser U, Boccaccini AR (2017) Regenerating bone with bioactive glass scaffolds: a review of in vivo studies in bone defect models. Acta Biomater 62:1–28

Evaluate (2015) EvaluateMedTech® – world preview 2015, Outlook to 2020. www.evaluategroup.com

Felzmann R, Gruber S, Mitteramskogler G, Tesavibul P, Boccaccini AR, Liska R, Stampfl J (2012) Lithography-based additive manufacturing of cellular ceramic structures. Adv Eng Mater 14:1052–1058

Ghosh SK, Nandi SK, Kundu B, Datta S, De DK, Roy SK, Basu D (2008) In vivo response of porous hydroxyapatite and β-tricalcium phosphate prepared by aqueous solution combustion method and comparison with bioglass scaffolds. J Biomed Mater Res B Appl Biomater 86:217–227

Guo J, Meng Z, Chen G, Xie D, Chen Y, Wang H, Tang W, Liu L, Jing W, Long J, Guo W, Tian W (2012) Restoration of critical-size defects in the rabbit mandible using porous nanohydroxyapatite-polyamide scaffolds. Tissue Eng A 18:1239–1252

Habibovic P, Gbureck U, Doillon CJ, Bassett DC, van Blitterswijk CA, Barralet JE (2008) Osteoconduction and osteoinduction of low-temperature 3D printed bioceramic implants. Biomaterials 29:944–953

Hannouche D, Hamadouche M, Nizard R, Bizot P, Meunier A, Sedel L (2005) Ceramics in total hip replacement. Clin Orthop Relat Res:62–71

Hench LL (2006) The story of Bioglass®. J Mater Sci Mater Med 17:967–978

Hench LL, Wilson J (2013) Introduction. In: Hench LL (ed) An introduction to bioceramics, 2nd edn. Imperial College Press, London, pp 1–26

Hing KA, Annaz B, Saeed S, Revell PA, Buckland T (2005) Microporosity enhances bioactivity of synthetic bone graft substitutes. J Mater Sci Mater Med 16:467–475

Igawa K, Mochizuki M, Sugimori O, Shimizu K, Yamazawa K, Kawaguchi H, Nakamura K, Takato T, Nishimura R, Suzuki S, Anzai M, Chung U Il, Sasaki N (2006) Tailor-made tricalcium phosphate bone implant directly fabricated by a three-dimensional ink-jet printer. J Artif Organs 9:234–240

Inzana JA, Olvera D, Fuller SM, Kelly JP, Graeve OA, Schwarz EM, Kates SL, Awad HA (2014) 3D printing of composite calcium phosphate and collagen scaffolds for bone regeneration. Biomaterials 35:4026–4034

ISO/ASTM 52900 (2015) Additive manufacturing – general principles – terminology. ISO Central Secretariat, Geneva

Jahadakbar A, Shayesteh Moghaddam N, Amerinatanzi A, Dean D, Karaca H, Elahinia M (2016) Finite element simulation and additive manufacturing of stiffness-matched NiTi fixation hardware for mandibular reconstruction surgery. Bioengineering 3:36

Jaiswal AK, Dhumal RV, Ghosh S, Chaudhari P, Nemani H, Soni VP, Vanage GR, Bellare JR (2013) Bone healing evaluation of nanofibrous composite scaffolds in rat calvarial defects: a comparative study. J Biomed Nanotechnol 9:2073–2085

Jakus AE, Rutz AL, Jordan SW, Kannan A, Mitchell SM, Yun C, Koube KD, Yoo SC, Whiteley HE, Richter CP, Galiano RD (2016) Hyperelastic bone: A highly versatile, growth factor-free, osteoregenerative, scalable, and surgically friendly biomaterial. Science translational medicine 8:358

Jakus AE, Ramille S (2017) Multi and mixed 3D-printing of graphene-hydroxyapatite hybrid materials for complex tissue engineering. J Biomed Mater Res A 105:274–283

Ji W, Sun Y, Yang F, Van Den Beucken JJJP, Fan M, Chen Z, Jansen JA (2011) Bioactive electrospun scaffolds delivering growth factors and genes for tissue engineering applications. Pharm Res 28:1259–1272

Keller TS (1994) Predicting the compressive mechanical behavior of bone. J Biomech 27:1159–1168

Kelly JR, Nishimura I, Campbell SD (1996) Ceramics in dentistry: historical roots and current perspectives. J Prosthet Dent 75:18–32

Kingery WD, Bowen HK, Uhlmann DR (1976) Introduction to ceramics, 2nd edn. Wiley, New York, p 3

Kurien T, Pearson RG, Scammell BE (2013) Bone graft substitutes currently available in orthopaedic practice: the evidence for their use. Bone Joint J 95B:583–597

Larsen M, Mishra R, Miller M, Dean D (2015) Bioprinting of bone. In: Atala A, Yoo JJ (eds) Essentials of 3D biofabrication and translation. Academic press (Elsevier), Cambridge, MA, pp 293–308

Learmonth ID, Young C, Rorabeck C (2007) The operation of the century: total hip replacement. Lancet 370:1508–1519

Li Z, Chen X, Zhao N, Dong H, Li Y, Lin C (2013) Stiff macro-porous bioactive glass-ceramic scaffold: fabrication by rapid prototyping template, characterization and in vitro bioactivity. Mater Chem Phys 141:76–80

Li Y, Chen SK, Li L, Qin L, Wang XL, Lai YX (2015) Bone defect animal models for testing efficacy of bone substitute biomaterials. J Orthop Transl 3:95–104

Li JJ, Roohani-Esfahani S-I, Dunstan CR, Quach T, Steck R, Saifzadeh S, Pivonka P, Zreiqat H (2016) Efficacy of novel synthetic bone substitutes in the reconstruction of large segmental bone defects in sheep tibiae. Biomed Mater 11:15016

Liu Y, Lim J, Teoh SH (2013) Review: development of clinically relevant scaffolds for vascularised bone tissue engineering. Biotechnol Adv 31:688–705

Liu W-C, Robu IS, Patel R, Leu MC, Velez M, Gabriel Chu T-M (2014) The effects of 3D bioactive glass scaffolds and BMP-2 on bone formation in rat femoral critical size defects and adjacent bones. Biomed Mater 9(45013)

Lohfeld S, Cahill S, Barron V, McHugh P, Dürselen L, Kreja L, Bausewein C, Ignatius A (2012) Fabrication, mechanical and in vivo performance of polycaprolactone/tricalcium phosphate composite scaffolds. Acta Biomater 8:3446–3456

Marcacci M, Kon E, Moukhachev V, Lavroukov A, Kutepov S, Quarto R, Mastrogiacomo M, Cancedda R (2007) Stem cells associated with macroporous bioceramics for long bone repair: 6- to 7-year outcome of a pilot clinical study. Tissue Eng 13:947–955

McColm IJ (2013) Dictionary of ceramic science and engineering. Springer, New York, pp 83–84

Metsger DS, Driskell TD, Paulsrud JR (1982) Tricalcium phosphate ceramic – a resorbable bone implant: review and current status. J Am Dent Assoc 105:1035–1038

Midha S, Kim TB, Van Den Bergh W, Lee PD, Jones JR, Mitchell CA (2013) Preconditioned 70S30C bioactive glass foams promote osteogenesis in vivo. Acta Biomater 9:9169–9182

Miranda P, Pajares A, Saiz E, Tomsia AP, Guiberteau F (2008) Mechanical properties of calcium phosphate scaffolds fabricated by robocasting. J Biomed Mater Res A 85:218–227

Moghaddam NS, Skoracki R, Miller M, Elahinia M, Dean D (2016a) Three dimensional printing of stiffness-tuned, nitinol skeletal fixation hardware with an example of mandibular segmental defect repair. Procedia CIRP 49:45–50

Moghaddam N, Jahadakbar A, Amerinatanzi A, Elahinia M, Miller M, Dean D (2016b) Metallic fixation of mandibular segmental defects. Plast Reconstr Surg Glob Open 4:e858

Muller B, Reseland JE, Haugen HJ, Tiainen H (2015) Cell growth on pore-graded biomimetic TiO2 bone scaffolds. J Biomater Appl 29:1284–1295

Nandi SK, Kundu B, Datta S, De DK, Basu D (2009) The repair of segmental bone defects with porous bioglass: an experimental study in goat. Res Vet Sci 86:162–173

Nie L, Chen D, Fu J, Yang S, Hou R, Suo J (2015) Macroporous biphasic calcium phosphate scaffolds reinforced by poly-L-lactic acid/hydroxyapatite nanocomposite coatings for bone regeneration. Biochem Eng J 98:29–37

Obregon F, Vaquette C, Ivanovski S, Hutmacher DW, Bertassoni LE (2015) Three-dimensional bioprinting for regenerative dentistry and craniofacial tissue engineering. J Dent Res 94:143S–152S

Paderni S, Terzi S, Amendola L (2009) Major bone defect treatment with an osteoconductive bone substitute. Musculoskelet Surg 93:89–96

Park HJ, Min KD, Lee MC, Kim SH, Lee OJ, Ju HW, Moon BM, Lee JM, Park YR, Kim DW, Jeong JY, Park CH (2016) Fabrication of 3D porous SF/β-TCP hybrid scaffolds for bone tissue reconstruction. J Biomed Mater Res A:1779–1787

Pati F, Jang J, Lee JW, Cho D-W (2015) Extrusion bioprinting. In: Atala A, Yoo JJ (eds) Essentials of 3D biofabrication and translation. Academic, Boston, pp 123–152

Pearce AI, Richards RG, Milz S, Schneider E, Pearce SG (2007) Animal models for implant biomaterial research in bone: a review. Eur Cells Mater 13:1–10

Piconi C, Maccauro G (1999) Zirconia as a ceramic biomaterial. Biomaterials 20:1–25

Pilipchuk SP, Plonka AB, Monje A, Taut AD, Lanis A, Kang B, Giannobile WV (2015) Tissue engineering for bone regeneration and osseointegration in the oral cavity. Dent Mater 31:317–338

Policastro GM, Lin F, Smith Callahan LA, Esterle A, Graham M, Stakleff KS, Becker ML (2015) OGP functionalized phenylalanine-based poly(ester urea) for enhancing osteoinductive potential of human mesenchymal stem cells. Biomacromolecules 16:1358–1371

Pountos I, Giannoudis PV (2016) Is there a role of coral bone substitutes in bone repair? Injury 47:2606–2613

Qiu K, Chen B, Nie W, Zhou X, Feng W, Wang W, Chen L, Mo X, Wei Y, He C (2016) Electrophoretic deposition of dexamethasone-loaded mesoporous silica nanoparticles onto poly(l-lactic acid)/poly(ε-caprolactone) composite scaffold for bone tissue engineering. ACS Appl Mater Interfaces 8:4137–4148

Quarto R, Mastrogiacomo M, Cancedda R, Kutepov SM, Mukhachev V, Lavroukov A, Kon E, Marcacci M (2001) Repair of large bone defects with the use of autologous bone marrow stromal cells. N Engl J Med 344:385–386

Raman R, Bashir R (2015) Stereolithographic 3D bioprinting for biomedical applications. In: Atala A, Yoo JJ (eds) Essentials of 3D biofabrication and translation. Academic press (Elsevier), Cambridge, MA, pp 89–121

Reichert JC, Wullschleger ME, Cipitria A, Lienau J, Cheng TK, Schütz MA, Duda GN, Nöth U, Eulert J, Hutmacher DW (2011) Custom-made composite scaffolds for segmental defect repair in long bones. Int Orthop 35:1229–1236

Ren J, Blackwood KA, Doustgani A, Poh PP, Steck R, Stevens MM, Woodruff MA (2014) Melt-electrospun polycaprolactone strontium-substituted bioactive glass scaffolds for bone regeneration. J Biomed Mater Res A 102:3140–3153

Schmitz JP, Hollinger JO (1986) The critical size defect as an experimental model for craniomandibulofacial nonunions. Clin Orthop Relat Res 205:299–308

Semlitsch M, Lehmann M, Weber H, Doerre E, Willert HG (1977) New prospects for a prolonged functional lifespan of artificial hip joints by using the material combination polyethylene/aluminium oxide ceramic/metal. J Biomed Mater Res 11:537–552

Shao H, He Y, Fu J, He D, Yang X, Xie J, Yao C, Ye J, Xu S, Gou Z (2016) 3D printing magnesium-doped wollastonite/β-TCP bioceramics scaffolds with high strength and adjustable degradation. J Eur Ceram Soc 36:1495–1503

Shrivats AR, Alvarez P, Schutte L, Hollinger JO (2014) Bone regeneration. In: Principles of tissue engineering. Elsevier, San Diego, pp 1201–1221

Sing SL, Yeong WY, Wiria FE, Tay BY, Zhao Z, Zhao L, Tian Z, Yang S (2017) Direct selective laser sintering and melting of ceramics: a review. Rapid Prototyp J 23:611–623

Sun M, Liu A, Shao H, Yang X, Ma C, Yan S, Liu Y, He Y, Gou Z (2016) Systematical evaluation of mechanically strong 3d printed diluted magnesium doping wollastonite scaffolds on osteogenic capacity in rabbit calvarial defects. Sci Rep 6:34029

Tamjid E, Simchi A (2015) Fabrication of a highly ordered hierarchically designed porous nanocomposite via indirect 3D printing: mechanical properties and in vitro cell responses. Mater Des 88:924–931

Tang W, Policastro GM, Hua G, Guo K, Zhou J, Wesdemiotis C, Doll GL, Becker ML (2014) Bioactive surface modification of metal oxides via catechol-bearing modular peptides: multivalent-binding, surface retention, and peptide bioactivity. J Am Chem Soc 136:16357–16367

Tang W, Lin D, Yu Y, Niu H, Guo H, Yuan Y, Liu C (2016) Bioinspired trimodal macro/micro/nanoporous scaffolds loading rhBMP-2 for complete regeneration of critical size bone defect. Acta Biomater 32:309–323

Tarafder S, Balla VK, Davies NM, Bandyopadhyay A, Bose S (2013) Microwave-sintered 3D printed tricalcium phosphate scaffolds for bone tissue engineering. J Tissue Eng Regen Med 7:631–641

Tesavibul P, Felzmann R, Gruber S, Liska R, Thompson I, Boccaccini AR, Stampfl J (2012) Processing of 45S5 Bioglass® by lithography-based additive manufacturing. Mater Lett 74:81–84

Vivanco J, Aiyangar A, Araneda A, Ploeg HL (2012) Mechanical characterization of injection-molded macro porous bioceramic bone scaffolds. J Mech Behav Biomed Mater 9:137–152

Wang H, Li Y, Zuo Y, Li J, Ma S, Cheng L (2007) Biocompatibility and osteogenesis of biomimetic nano-hydroxyapatite/polyamide composite scaffolds for bone tissue engineering. Biomaterials 28:3338–3348

Woodruff MA, Lange C, Reichert J, Berner A, Chen F, Fratzl P, Schantz JT, Hutmacher DW (2012) Bone tissue engineering: from bench to bedside. Mater Today 15:430–435

Xu Y, Luong D, Walker JM, Dean D, Becker ML (2017) Modification of poly (propylene fumarate) – bioglass composites with peptide conjugates to enhance bioactivity. Biomacromolecules 18:3168–3177

Yuan H, Fernandes H, Habibovic P, de Boer J, Barradas AMC, de Ruiter A, Walsh WR, van Blitterswijk CA, de Bruijn JD (2010) Osteoinductive ceramics as a synthetic alternative to autologous bone grafting. Proc Natl Acad Sci USA 107:13614–13619

Zanchetta E, Cattaldo M, Franchin G, Schwentenwein M, Homa J, Brusatin G, Colombo P (2016) Stereolithography of SiOC ceramic microcomponents. Adv Mater 28:370–376

Zhang J, Liu H, Ding J-X, Wu J, Zhuang X-L, Chen X-S, Wang J-C, Yin J-B, Li Z-M (2016) High-pressure compression-molded porous resorbable polymer/hydroxyapatite composite scaffold for cranial bone regeneration. ACS Biomater Sci Eng 2:1471–1482

Zhou C, Ye X, Fan Y, Ma L, Tan Y, Qing F, Zhang X (2014) Biomimetic fabrication of a three-level hierarchical calcium phosphate/collagen/hydroxyapatite scaffold for bone tissue engineering. Biofabrication 6:35013

Zocca A, Colombo P, Gomes CM, Günster J (2015) Additive manufacturing of ceramics: issues, potentialities, and opportunities. J Am Ceram Soc 98:1983–2001

Zoetis T, Tassinari MS, Bagi C, Walthall K, Hurtt ME (2003) Species comparison of postnatal bone growth and development. Birth Defects Res B Dev Reprod Toxicol 68:86–110

Zreiqat H, Ramaswamy Y, Wu C, Paschalidis A, Lu Z, James B, Birke O, McDonald M, Little D, Dunstan CR (2010) The incorporation of strontium and zinc into a calcium-silicon ceramic for bone tissue engineering. Biomaterials 31:3175–3184